Modeling battery cells with different chemistries based on EIS measurements

Benedek Marot s2632853
University of Twente - Power Electronics Group
EEMCS faculty
June 28, 2024

I. Abstract

***Abstract*—In the rapidly growing need for clean and green energy, the market for batteries is growing fast. The research for better performance, longer lifetime and higher storage capacity is one of the most important topics in the battery sector. To further improve battery technologies, modelling and simulation are indispensable. To successfully simulate and model batteries, equivalent circuit models (ECM) need to be developed. In this report, three different Lithium-ion battery chemistries are investigated and their potential ECM is discussed. With the help of EIS measurements, impedance plots can be obtained for each battery type, from these plots different conclusions are drawn regarding the relationship between impedance and state of charge (SoC) and between impedance and charging direction. After these, the potential ECMs were simulated and compared to the measurement data. It turned out that for two of the three chemistries, the same ECM is a suitable choice. This ECM included two CPEs, resistors and a Warburg element.**

II. Introduction

In today's world, the field of power electronics is a very important and innovative one. As there is more and more need for energy and energy storage. The demand for batteries has been rising significantly over the last couple of years. The need for high-performance rechargeable batteries is at an all-time high. One of the most used battery types today is the Lithium-ion battery. Lithium-ion batteries are the fastest-growing and most promising battery chemistry in today's market. Similar to most technologies, Lithium-ion batteries have advantages and disadvantages. The advantages include high energy density, low self-discharge rate, low maintenance need, high cell voltage and good load characteristics. These are mostly why Lithium-ion batteries are starting to replace other battery types such as Nickel-Cadmium or lead-acid on the battery market. On the other hand, there are disadvantages to this type of battery. These are the need for protection circuits and ageing [1] [2]. These are the reasons that the decision was made to do this project and to potentially start to decrease the disadvantages of Lithium-ion batteries. The first lithium-ion battery was created and commercialised by Sony about 35 years ago. Since then intensive research has been done to improve the design of these batteries. Some ongoing research topics for Li-ion batteries are recycling, extending battery life, cost reduction and safety improvements. A massive increase in the research happened around the 2010s when the importance of environmental safety and emissions reduction increased significantly.

The market for lithium-ion batteries is also increasing and projections show that it will increase even further in the near future. This means that market experts project that the required battery power will increase to 4.7 TWh by 2030 from the 700 GWh required in 2022. This would indicate a 30% increase annually in battery power demand [3]. This growth is mainly driven by two major driver:

- A shift towards sustainability, which includes the ban on combustion engines and the increased demand for electric vehicles.
- Increased consumer demand for greener technologies.

One estimate is that by 2030 the value of the global Lithium-ion battery market will reach more than $184 billion, which was $48.8 billion in 2022. This would mean that by 2030 there would be an 18.5% annual increase in value [4].

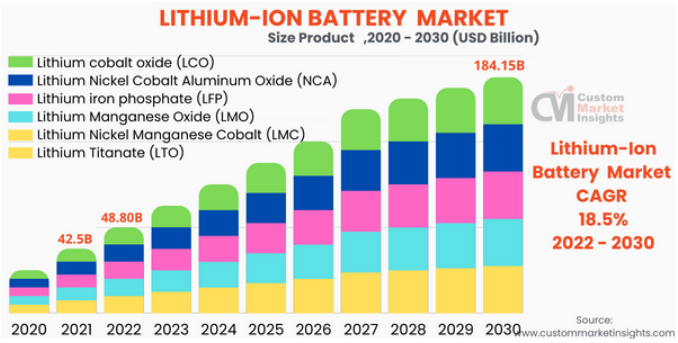

Fig. 1: Lithium-ion battery market projections [4]

A. Research Question

As one can see on fig. 1, there are multiple chemistries used in lithium-ion batteries. The five most common technologies are the followings:

- LFP: Lithium-Iron Phosphate
- NMC: Lithium Nickel Manganese Cobalt Oxide
- LMO: Lithium Manganese Oxide
- NCA: Lithium Nickel Cobal Aluminium
- LTO: Lithium Titanate

Researchers can make equivalent circuit models (ECM) of the specific chemistries and measure the performance of these models. Multiple ECMs exist for different technologies. The technology called Electrochemical Impedance Spectroscopy (EIS) will be utilized to measure cell performance, and from these measurements, impedance-based ECMs will be created. In this paper, the measured data will be analysed and a comparison will be presented between some of the above-mentioned chemistry technologies and their ECMs. The goal of the comparison is to obtain the best-performing ECM of the chosen chemistries. This will be done by measuring the impedance of actual battery cells, selecting a potential ECM, identifying the parameters of the circuit and then verifying the accuracy of the ECMs. Finally, a comparison will be made where the differences will be discussed between the different chemistries.

The structure of the paper is the following. In section III, a literature review on the battery electrochemical mechanisms, battery characteristics, impedance performance and equivalent circuit models is conducted. In section IV, the measurement set-up for obtaining battery impedance is described. The experimental analysis and the choice of ECMs are presented in section V and the conclusion is presented in section VI.

III. Theory and Literature Review

A. Lithium-Ion batteries

1) How do they work?

In this paragraph the basics of Lithium-ion batteries will be discussed. A typical Li-ion battery consists of [5] [6]:

- **Electrolyte:** The charged ends of a cell, which are attached to the current collectors
- **Anode:** The negative electrode
- **Cathode:** The positive electrode
- **Electrolyte:** A liquid, gel or polymer that conducts electricity
- **Separator:** Typically a microporous polymer membrane that separates the electrodes, while allowing the exchange of lithium ions between the two electrodes

One can see how a Li-ion battery is designed and what components it includes on fig. 2.

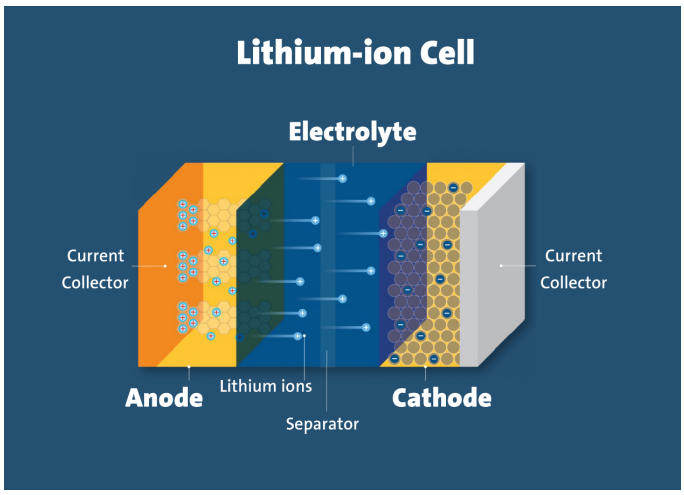

Fig. 2: Components of a Li-ion battery [5]

The working method of these batteries can be described as such: the Lithium ions move between the cathode and anode internally and electrons move in the opposite direction in the external circuit, which powers the external device. There are two states of a battery charging and discharging. When the battery is charging, the two electrodes are connected to an external supply. Hence, electrodes are forced to be released at the cathode and move externally to the anode. Simultaneously the lithium ions also move from the cathode to the anode. The opposite happens during the process of discharging. This time, the anode is the one that releases lithium ions to the cathode. This creates a flow of electrons which can power the connected device.

2) Cathode chemistry

The Lithium-ion battery is a specific type of battery by itself. However, there are different chemistry variations inside the category of Lithium-ion batteries. These variations come from the fact that the cathode and anode chemistry can change in every design. Most of the time the difference is in the cathode, the anode is usually the same. For the past 20 years, the preferred material for the anode has been graphite. They offer good Lithium transport, 2D mechanical stability and electrical conductivity [7]. There are multiple options to choose from regarding cathode chemistry. Some examples are

- Lithium-Iron Phosphate (LFP)
- Lithium Nickel Manganese Cobalt Oxide (NMC)
- Lithium Manganese Oxide (LMO)
- Lithium Nickel Aluminium (NCA)
- Lithium Titanate (LTO)

As mentioned before, the difference here is the chemistry of the cathode while the anode is graphite, except for the LTO, where the anode is a different material. On fig. 3 one can see the different technologies and what chemistries are utilised. Moreover, it can also be observed how they compare to each other in specific categories such as safety, power density and energy density.

The focus of this report is the comparison of the LFP, NMC and the LTO. The reason that these specific chemistries were chosen is that NMC is the most used battery in electric vehicles because of its high energy density. Moreover, LTO and LFP are the safest of them all and they have the potential to be used as energy storage systems for electric marine applications [8]. So it is important to take a look at these three battery chemistries in more detail.

Key Active Material	Lithium-Iron Phosphate	Lithium Nickel Manganese Cobalt Oxide	Lithium Manganese Oxide	Lithium Nickel Cobalt Aluminum	Lithium Titanate
Technology Short Name	LFP	NMC	LMO	NCA	LTO
Cathode	$LiFePO_4$	$LiNi_xMn_yCo_{z=x-y}O_2$	$LiMn_2O_{4(spinel)}$	$LiNiCoAlO_2$	variable
Anode	C (graphite)	C (graphite)	C (graphite)	C (graphite)	$Li_4Ti_5O_{12}$
Safety	▮▮▮▮	▮▮▮	▮▮▮▮	▮▮	▮▮▮▮
Power Density	▮▮▮	▮▮	▮▮▮▮	▮▮▮▮	▮▮▮▮
Energy Density	▮▮	▮▮▮▮	▮▮▮▮	▮▮▮▮	▮▮
Cell Costs Advantage	▮▮▮	▮▮▮	▮▮▮	▮	▮
Lifetime	▮▮▮▮	▮▮▮	▮▮▮	▮▮▮▮	▮▮▮▮
BESS Performance	▮▮▮▮	▮▮▮	▮▮▮	▮▮▮	▮▮▮▮

Fig. 3: Five different battery chemistry technologies [9]

a) LFP

These batteries could be a very good option to use when someone is looking for larger batteries, because of their long life-cycle and high safety. The advantages of this technology include exceptional safety features, they are non-toxic, they show no thermal runaway and they are chemically stable. Furthermore, they have a reasonably good energy density, they provide a strong power density and they are cost-effective. They are mostly used in commercial energy systems, electric vehicles or any other application that requires a long lifespan and high safety [9] [10].

b) NMC

The NMC battery is the most widely used Lithium-ion battery in electric vehicles. The main upside of this technology are the high energy density, lower toxicity and the low cost due to the usage of Manganese which is a cheaper material than Cobalt or Nickel. This type of battery can store more energy compared to others because of its high energy density. This combined with affordability makes them attractive for electric powertrains. Hence this type is mostly used in electric vehicles and bikes. The ability to tune the Nickel and Manganese content means that this technology can be optimised toward specific energy and power needs. This adaptability makes them useful in battery storage applications too [9] [11].

c) LTO

LTO is a bit different from the previously mentioned technologies. Here the graphite on the anode is replaced by lithium titanate as the active material. These batteries have extremely long lifetimes thanks to the zero volume change during lithiation. They are chemically stable, so safety is also excellent. The Lithium-titanate has a large surface area, which means that the number of electrons that can enter and exit the anode is extremely high. This enables fast charging and discharging. There are three main drawbacks regarding this type. These are that it has low nominal voltage and low energy density, so they perform poorly at high power levels. The final disadvantage is the cost. LTO is more expensive compared to other solutions because of the low worldwide production volume. Usually, these batteries are used in electric vehicles including electric buses. They are a good option for battery energy storage systems for storing wind and solar energy. They can potentially be used in aerospace applications [12] [13].

B. Equivalent circuit models

With the aim of safe operation and effectiveness of battery applications, modelling is very important. An equivalent circuit model or ECM is a model that is used to control and monitor

different Lithium-ion batteries. The goal of these ECMs is to simulate the internal characteristics of specific batteries. These circuits are created based on the existing physical and chemical knowledge of the chosen cell. Most of the time ECMs consist of resistor-capacitor (RC) pairs to replicate the internal behaviour of specific battery cells. One can connect multiple RC pairs to achieve more accurate approximations. An example of a first-order and second-order ECM can be seen on fig. 4. Theoretically, a second-order RC model should be more accurate, but it requires a higher computational complexity [14].

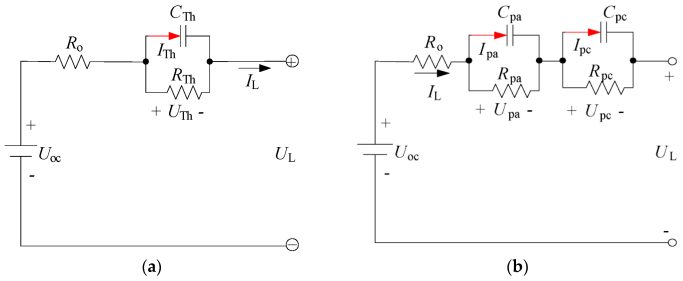

Fig. 4: First-order (1RC) and second-order (2RC) ECM examples [14]

One can see that multiple components are included in the circuits above. Namely, starting with the 1RC model:

- U_{OC}: Open-circuit voltage.
- R_O: Resistor for Ohmic resistance.
- R_{Th}: Resistor for polarization resistance.
- C_{Th}: Capacitance that outlines the battery's reaction while being charged and discharged.

The components in the 2RC model are:

- R_O: This represents the internal resistance component.
- R_{pa}: This mimics polarisation resistances.
- R_{pc}: A resistance for characterising concentration polarisation.
- C_{pa}: Capacitor to mirror the temporary reaction of the battery's charging/discharging cycle.
- C_{pc}: Capacitance to simulate polarisation traits.
- U_{OC}: Open-circuit voltage.

Realistically for EIS measurements, the ECMs will be a bit more complex than just the first- or second-order RC models. As mentioned before the second-order RC circuit is more accurate so the model for EIS could be an improved version of this. One could replace capacitances with Constant Phase Elements (CPE). Moreover, one or more Warburg elements (W) can be added to the circuit [15] [16]. This new model is called a fractional order ECM. A CPE is an element that can be used to describe the dispersion effect, but it can act as a resistor or a capacitor when α from eq. (1) is 0 or 1 respectively. The formula of the CPE element is the following:

$$Z_{CPE} = \frac{1}{(j\omega)^{\alpha} \cdot Q_{sei}} \tag{1}$$

The Warburg element (W) is important as this represents the diffusion mechanisms in the low-frequency region [17].

1) ECMs used for the different chemistry modelling

Circuits with CPEs or fractional order models, are widely used in modelling batteries. An example of a fractional model circuit can be seen on fig. 5. We can see the R-CPE pairs and a Warburg element at the end of the circuits.

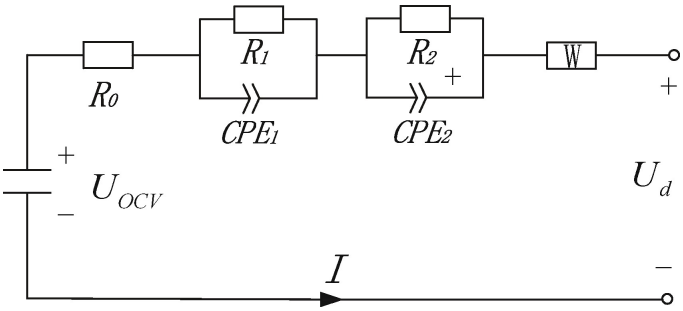

Fig. 5: Schematic of a potential fractional order equivalent circuit model. [16]

Many circuits can be used to model a Lithium-ion battery. The most used approach is to choose an ECM according to the shape of the impedance curve on the Nyquist plot. This plot can be obtained by performing the EIS measurement. There are three important regions of a battery that need modelling: the Ohmic region ($f > 1kHz$), Mid-frequency region ($1000Hz < f < 0.1Hz$) and Low-frequency region ($f < 0.1Hz$). Most of the time the Ohmic region is modelled by only a resistor. The difference between the models of the different battery chemistries is in the Mid-frequency and Low-frequency regions. The Mid-frequency region also includes two sub-regions, namely: Semiarch 1 and 2. These regions can be seen on fig. 6. Where options A and B can be potential ECM for LCO, option C might be good for NMC cells [17].

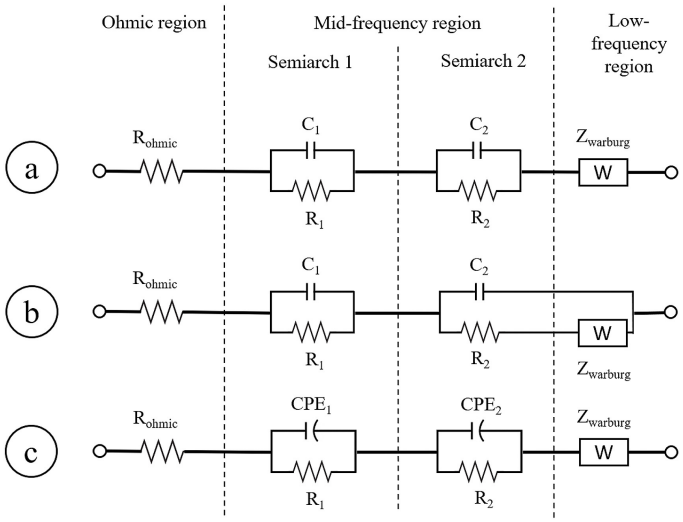

Fig. 6: Options to model the specific regions of a battery [17]

On table I, some of the possible options for ECMs are listed for NMC and LFP batteries. We can assume here that the Ohmic region was indeed modelled with a resistor. The symbols and abbreviations in table I represent the following:

- **-**: series connection.
- **//**: parallel connection.
- **RC**: parallel circuit of a resistor and a capacitor.
- **CPE**: constant phase element.
- **ZARC**: parallel circuit with a resistor and a constant phase element (CPE).
- **W**: Warburg element.
- **HN**: generalized ZARC
- **TLM**: transmission line

TABLE I: Comparison of Cathode Chemistry [17]

Cathode chemistry	Mid-frequency region		Low-frequency region
	Semiarich 1	Semiarich 2	
LFP	(R-W)//C		
LFP	ZARC		ZRAC
LFP	ZARC	ZARC	W
NMC	ZARC	ZARC-ZARC	
NMC	ZARC	TLM	
NMC	ZARC	ZARC	CPE
NMC	ZARC	ZARC	
NMC	ZARC	ZARC	W
NMC	ZARC	ZARC-CPE//(R-CPE)	
NMC	ZARC	CPE//(R-W)-CPE//(R-W)	
NMC	RC-RC	RC-RC	W
NMC	ZARC	ZARC	W
NMC	RC	RC	
NMC	ZARC-ZARC	TLM	
NMC	ZARC	CPE	
NMC	HN	HN	W
NMC	ZARC	ZARC	
NMC	RC		

For the LTO battery, the options for ECM are similar to the one mentioned before. One could use a second-order RC-pair ECM topology or the previously mentioned CPE circuits.

C. EIS performance on different battery chemistries

EIS is an effective tool to fit the ECM to the battery cells. Therefore it is necessary to look at the relationship between the State of Charge (SoC) and impedance for different battery chemistries and the relationship between impedance and charge/discharge directions at the same SoC. In this section these two topics will be discussed, the three chemistries mentioned are the LTO, NMC, and LFP.

1) Relationship between SoC and impedance of battery chemistries

For the LFP battery, the impedance is not heavily influenced in the mid-frequency region. This can be seen in previous publications by looking at the impedance graphs, where the impedance plots of different SoCs are very close in the first semi-circle. There is a significant difference in the low-frequency region, where the impedance plots split. The middle-frequency region of the SoC stays reasonably close together. However, the impedance is considerably different at 0% at 100% [18] [19]. LTO batteries have lower impedance than LFP and NMC. The impedance is similar in the middle-frequency region for the different SoCs, except the 0% at 100%. The impedance of these SoCs the impedance is already different compared to the others. This trend continues into the low-frequency region, the middle range of the SoC is resembling. The 0% at 100% is once again distinct [20]. These trends can be observed with the NMC battery too. In the middle-frequency region, the impedance of different SoCs is similar except the 0% at 100%. The same pattern can be detected in the low-frequency region [20].

2) Relationship between impedance and charge/discharge directions

Sometimes we can see that specific cells' OCV-SoC plots during charge and discharge are not exactly overlapping. This is caused by the phenomenon called hysteresis. To have a better understanding of the relationship between impedance and charging directions we have to look at the hysteresis of the mentioned battery cells. For the LTO cell, the expectation is that there is minimal to no hysteresis, so it is safe to say that the charging direction should not heavily influence the impedance [21]. According to literature, NMC can experience small hysteresis which can cause a minor difference in the impedance [22]. Hence, the expectation is that there will be a small difference in the impedance plots of charging and discharging for the NMC cell. The LFP cell has more significant hysteresis, note that this is still not extremely large but it is noticeable. The hysteresis effect is evident in this case, which means that there might be some visible differences between charging and discharging plots [23].

IV. Methodology & Experimental set-up

This section will present the methodology, description of measurement set-up and theory of the measurements. On fig. 7 we can see what the combined measurement set-up looks like. The cycling machine is on the left and the EIS machine is on the right side of the picture.

Fig. 7: Full measurement set-up

The experiment was performed for 2 different cells for the 3 different chemistry types, which means that 6 different battery cells were used in this project. The specific battery cells that were used in this project are LTO18650, NMC18650 and LFP18650. The experiment was then done for both charging and discharging directions. On fig. 8 one can see the full process of the measurement for the three cells NMC, LFP and LTO.

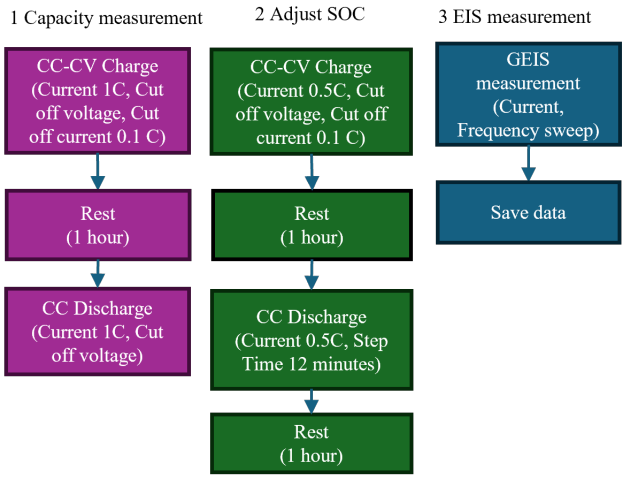

Fig. 8: Full measurement review

A. Electrochemical Impedance Spectroscopy

Electrochemical impedance spectroscopy or EIS technology is a measurement technology that is widely used to characterise specific Lithium-ion batteries. There are two significant modes of EIS. The first one is the galvanostatic mode (GEIS), where a sinusoidal current is applied of a certain frequency and amplitude. Then, this is repeated for multiple frequencies, which generates a characteristic impedance spectrum. The phase shift and the amplitude of the output voltage are measured. The other mode is the potentiostatic mode (PEIS) where the same methodology is used but instead of a sinusoidal current, a sinusoidal voltage is applied. For PEIS the output current of the circuit is measured. Both of these modes are a good option

to probe processes within the batteries. The output of these measurements can be plotted either into a Nyquist plot or a Bode plot. The plots offer the potential to parameterise the ECMs [24].

B. Testing architecture

1) EIS Measurement

The Solatron EchemLab XM is used for the EIS measurements, with an attached battery holder where the batteries were fixed during the measurement [25]. The RE pin is a reference pin that monitors voltage differences between the anode and cathode, the CE pin is connected to the anode of the cell and the WE pin is connected to the cathode of the cell. To get the measurement data and to parameterize the measurements a software called XM-Studio ECS is used. The type of the EIS experiment was chosen to be the galvanostatic impedance mode (GEIS).

It is important to choose the right current for these measurements. Hence the first measurement was to obtain the impedance graphs of the 3 cells with different currents. The most important part of this experiment is to see how the impedance of the cells changes based on the change in current. This is important because the current has to be high enough, to get better data quality, but not too high because then it would change the SoC of the cells. This was done by choosing an arbitrary frequency sweep from 100 mHz to 10 kHz, and then performing the GEIS measurement with different current amplitudes. On fig. 9, fig. 10 and fig. 11 we can see how the impedance changes based on the change in current for the three chemistries. We can see that the plotted NMC and LFP impedances are very consistent regardless of the current, so we can choose any of the shown currents and still get good data quality. On the other hand, for LTO we can see significant differences between different currents. The most noticeable is when the input amplitude is 10 mA, the plot shows that the data quality would be bad if one were to use this input, as the plotted impedance graph is not consistent with the others. The other currents are more similar to each other, we can see small deviance, however, this should not be a problem when choosing the current. Here we can also notice that the mid-frequency is almost the same for the remaining currents. The chosen current for NMC is 80 mA, for LFP it is 60 mA and for LTO it is 80 mA. The chosen frequency for the sweep was 20 mHz-20 kHz, as this sweep gives a good range in frequency to properly analyse the generated plots.

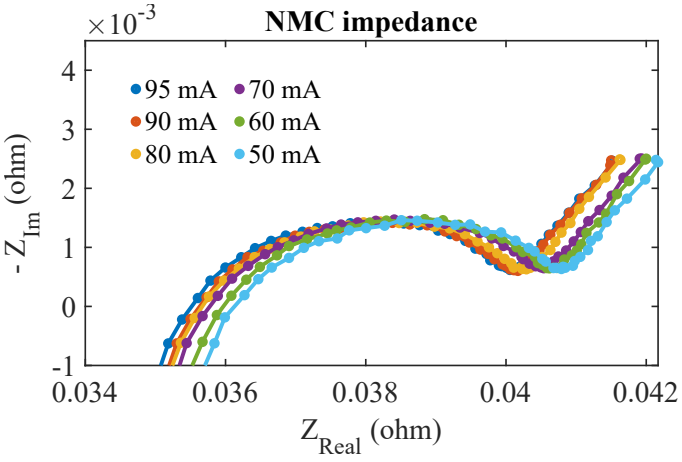

Fig. 9: NMC impedance with different currents

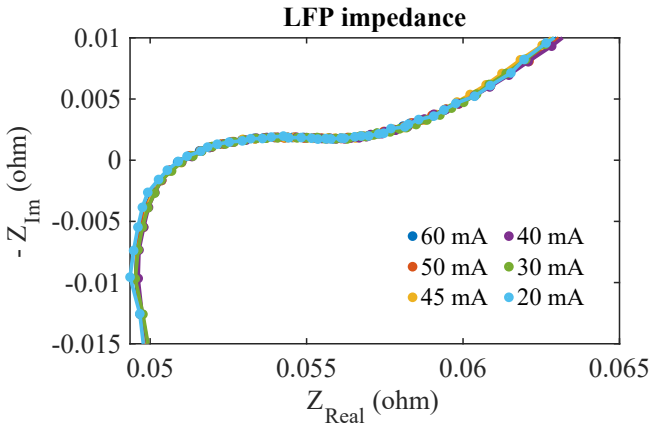

Fig. 10: LFP impedance with different currents

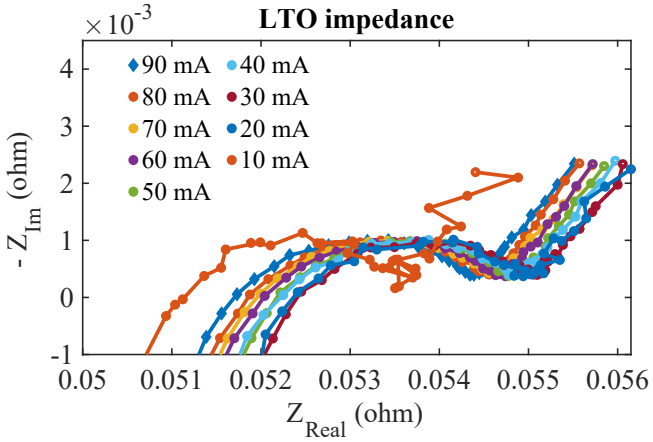

Fig. 11: LTO impedance with different currents

2) Capacity measurement

Battery cycling, which means changing the SoC of the cells by charging or discharging, is done with the Arbin RBT (0-60 V) cycler. This machine has 4 channels so we could modify the SoC of 4 battery cells at the same time. The software used for setting the parameters is the Mits Pro. Here an object file had to be created where specifics about the battery cells had to be provided. Additionally, a schedule file was needed that specifies the steps of the cycling. The object files for the 3 cells were done with the help of the datasheet for the cells. To complete the schedule files, the preparation of the cells had to be completed and the full battery capacity of the cells had to be obtained. For preparation three full charge and full discharge cycles had to be done. The schedule files for the three cells were constructed in the following way:

- Charge to a 100 %: Constant Current Constant Voltage (CCCV) function that charges the cell with 0.5C, based on the datasheet, until the voltage is less than equal to $0.05 \cdot NominalCapacity$.
- Resting time of one hour so the cell becomes relaxed and the voltage becomes constant.
- Discharge with 0.5C until the specific minimum voltage is provided by the datasheet of the cells.

This cycle was done three times for each chemistry and both of the cells of the chemistries. After this experiment was conducted the capacity for each cell was obtained:

- NMC1: 2.474 Ah
- NMC2: 2.433 Ah
- LTO1: 1.489 Ah
- LTO2: 1.486 Ah
- LFP1: 1.772 Ah
- LFP2: 1.8 Ah

From the capacity values, the charging and discharging current could be acquired. For safety, it was decided to use 0.5C

as the current value. After the capacities were obtained, the cycling and EIS were combined into one measurement setup.

3) Combined measurement set-up

The actual measurement was the combination of the two devices mentioned above with an extra Keithley DAQ6510 multimeter system. There are some changes compared to the previously described setups. The battery holder was removed, and the multimeter was connected to the EIS machine, the battery and the cycling machine. The cycling machine was responsible for the SoC modification, the EIS machine for the EIS measurement and the multimeter for the switching between the two. With this setup, there is no need to unnecessarily move the battery cells as this would most likely give false results. To change the SoC of the cells a new schedule file was constructed. These included a charge or discharge cycle with 0.5C, based on the capacity measurements, for 12 minutes to change 10 % of SoC. Following the modification of the SoC, a one-hour rest time was included to relax the chemistry of the battery cell. The method of the measurement was the following:

- Increase/decrease 10 % of the SoC
- Rest the cells for one hour
- Switch the connection from cycling to EIS with the multimeter
- Perform the EIS measurement
- Obtain EIS data using the software
- Switch back to cycling using the multimeter

V. Results and Discussion

In this section, the obtained result and their analysis will be discussed. Moreover, the process of choosing a suitable ECM and the validation of this choice will be explained.

A. Experimental analysis

1) Relationship between SoC and impedance

The described experiment in section IV-B3 was performed on the battery cells of the three chemistries. The same sequence of experiments was performed during discharging and charging.

a) LTO

First, the impedance of the LTO cells was produced, with the same set of experiments as mentioned in section IV. On fig. 12 and fig. 13 we can see the LTO cell's impedance during charge and discharge.

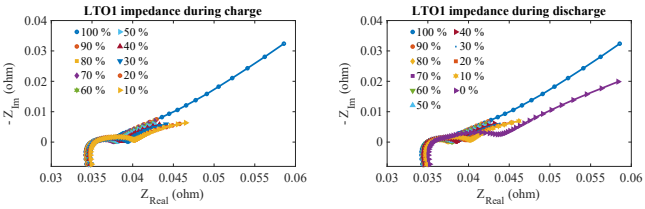

Fig. 12: Left: LTO1 impedance during charge. Right: LTO1 impedance during discharge

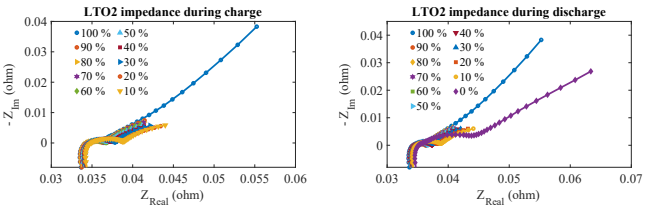

Fig. 13: Left: LTO2 impedance during charge. Right: LTO2 impedance during discharge

One can see that the Nyquist plots do not change drastically on different SoCs. It is noticeable that 100% and 0% SoC are the only distinguishable impedances. These have significantly higher impedance compared to the others. Other than these, the impedances are close to each other, they are almost identical in the mid-frequency region, but there are slight differences in the low-frequency region. One can also observe that the real part of the impedance is decreasing with the SoC increasing. Moreover, the imaginary part of the battery impedance is increasing as the SoC is increasing too. These trends can be identified for the two cells and the charging directions. In conclusion, we can say that LTO cells have higher impedance when full or empty, the impedance slightly decreases when the SoC is increasing and the impedances are very similar between 0% and 100%.

b) NMC

The next battery chemistry to analyse was the NMC. On fig. 14 and fig. 15 we can see the Nyquist plots of the impedance for two different NMC cells during charge and discharge respectively.

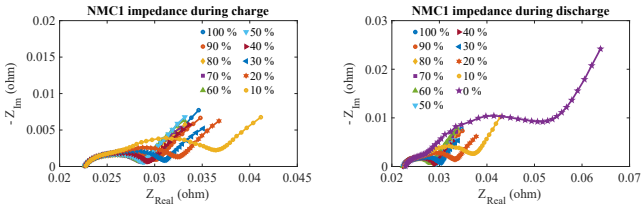

Fig. 14: Left: NMC1 Impedance during charge. Right: NMC1 Impedance during discharge

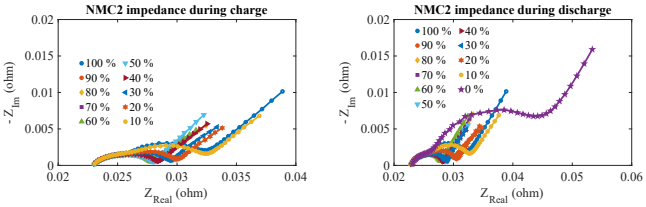

Fig. 15: Left: NMC2 Impedance during charge. Right: NMC2 impedance during discharge

The graphs show that NMC is similar to LTO in terms of the relationship between SoC and impedance. We can see from the graphs that the mid-frequency impedance is very similar at every SoC, this can be seen by the fact that the first semi-arch of the impedances are very close to each other. It can also be said that the biggest change in the impedance is at 0%, 10% and 20% for both charging and discharging. We can conclude from the graphs, that the impedances are higher when the SoC is lower and start to decrease around 30%. This can be proved by noticing that the corresponding plot to these SoC values is more to the right on the x-axis, meaning a higher real impedance value and further up on the y-axis, meaning a higher imaginary impedance. We can also see that the real part impedance starts to decrease as the SoC increases and the imaginary part almost stays constant. Moreover, it is also apparent that the difference between the two cells is negligible. In summary, the real impedance of the higher SoCs is lower and the overall impedance plots have very similar characteristics regardless of the charging direction and the SoC.

c) LFP

Finally, the LFP battery cell was investigated. On fig. 16 and fig. 17 we can see the impedance of the two LFP cells during charging and discharging.

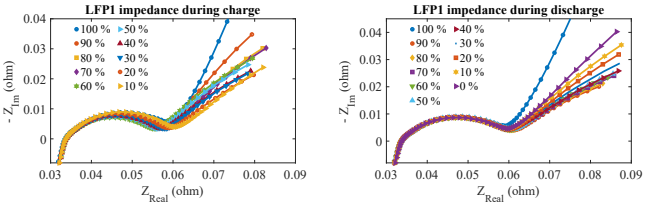

Fig. 16: Left: LFP1 Impedance during charge. Right: LFP1 Impedance during discharge

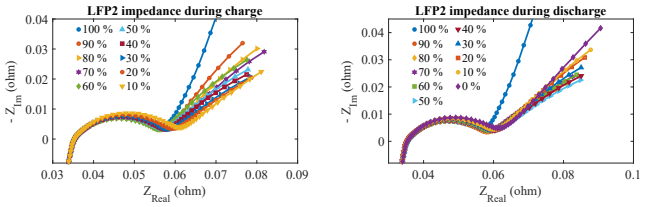

Fig. 17: Left: LFP2 Impedance during charge. Right: LFP2 impedance during discharge

The plots are similar to the previous cells in terms of they are comparable to each other. One can see that the trends are alike. The mid-frequency region is almost identical for every SoC regardless of the cell and charging direction. The differences are in the low-frequency region. We can see that 100% SoC has a significantly different impedance plot for the two cells during charge and discharge. Interestingly we can see a distinct trend in how the value of the impedance changes. For both cells during charge, the impedance shows a decreasing trend, apart from 100%, the higher the SoC is the lower the impedance is. This is exactly the opposite during charging. Once again ignoring the 100%, we can see that the impedance increases as SoC increases. After this analysis, we can say that SoC does not influence the impedance in a major way. From these plots, we can already deduce that the impedance is influenced by the charging direction but more about this in section V-A2.

d) Same frequency comparison

To further prove the conclusion that the impedance is not dependent on the SoC a final graph was constructed. Two specific frequencies were chosen, one higher (2000 Hz) and one lower (1 Hz). After this, the real impedance and imaginary impedance data from every SoC was collected. The assumption is that on the plots the impedance of the high-frequency region will be lower than the low-frequency region, as on the impedance plot this part is more on the left, hence the lower value. This assumption is proved by looking at the graphs as this is exactly what we see. The plots show how the impedances change with the SoC for a specific frequency. On fig. 18 and fig. 19 we can see the graphs for the real and imaginary impedance respectively. There are different conclusions we can draw from this. These can be

- **LTO:** For this battery cell it is apparent that the real part of the impedance is unaffected by the SoC for high frequencies and there is a slight decrease as the SoC increases. These can be seen from the straightness of the line, but also one can notice a decreasing trend of the line. This however is almost negligible. For low frequency, the same trend can be realised. This time it is more significant as there is a higher deviation in impedance. Similarly, the imaginary impedance is almost constant at the high frequency. At low frequency, the imaginary impedance is also close to a straight line, there is a small change at 0% and 100%.
- **NMC:** We can see similar trends for NMC as for LTO. For higher frequencies, the line is almost completely straight meaning that the SoC level does not heavily influence the impedance. The decreasing trend can also be noticed, meaning that the higher the frequency the lower the impedance is. For lower frequencies, the decline is once again bigger. The imaginary impedance at high frequency is steady regardless of the SoC. At low frequency, there is an increase until 30% but after that the impedance is unvarying.
- **LFP:** For the LFP the basic trends are similar to the other two cells. The real impedance of this cell is almost a straight line for both high and low frequencies. We can say that SoC does not influence the real impedance of the LFP cell. Similarly, it can be observed that for high frequency the plot is almost straight. However, for the low frequency, we can see that the line is consistent until the 90% SoC and then there is a sudden decrease. This can be explained by the fact that the impedance of the 100% is significantly different at the low-frequency region compared to the other SoCs. This is nicely visualized in this graph too.

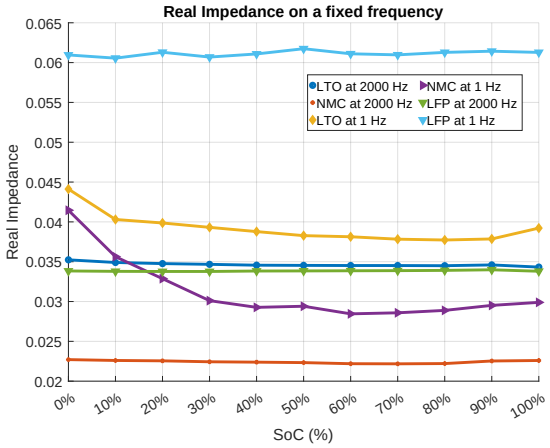

Fig. 18: Real impedance of the battery cells at specific frequencies

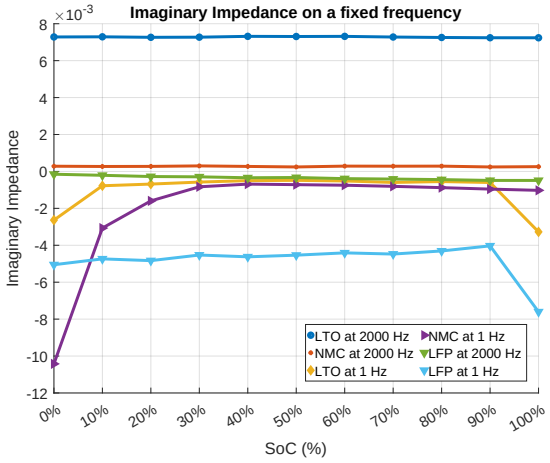

Fig. 19: Imaginary impedance of the battery cells at specific frequencies

As a conclusion for this paragraph, we can say that the SoC does not influence the real or imaginary impedance of the three cells. Hence, we can assume that this is the case for the actual impedance too. We can then say that the SoC does not influence the impedance of the cells.

2) Influence of charging and discharging direction

After the relationship between impedance and SoC was acknowledged, it is important to look at how the charging and discharging direction influences the impedance on a specific impedance. Three SoC was chosen, namely 10%, 50% and 90%, to show how the impedance changes. As mentioned and shown before, the cells have very congruent impedances. Hence, from now on we will assume that we can deduce results from only one of the cells, namely LTO1, NMC1 and LFP1. On fig. 20 we can see the impedance plots for the three chemistries.

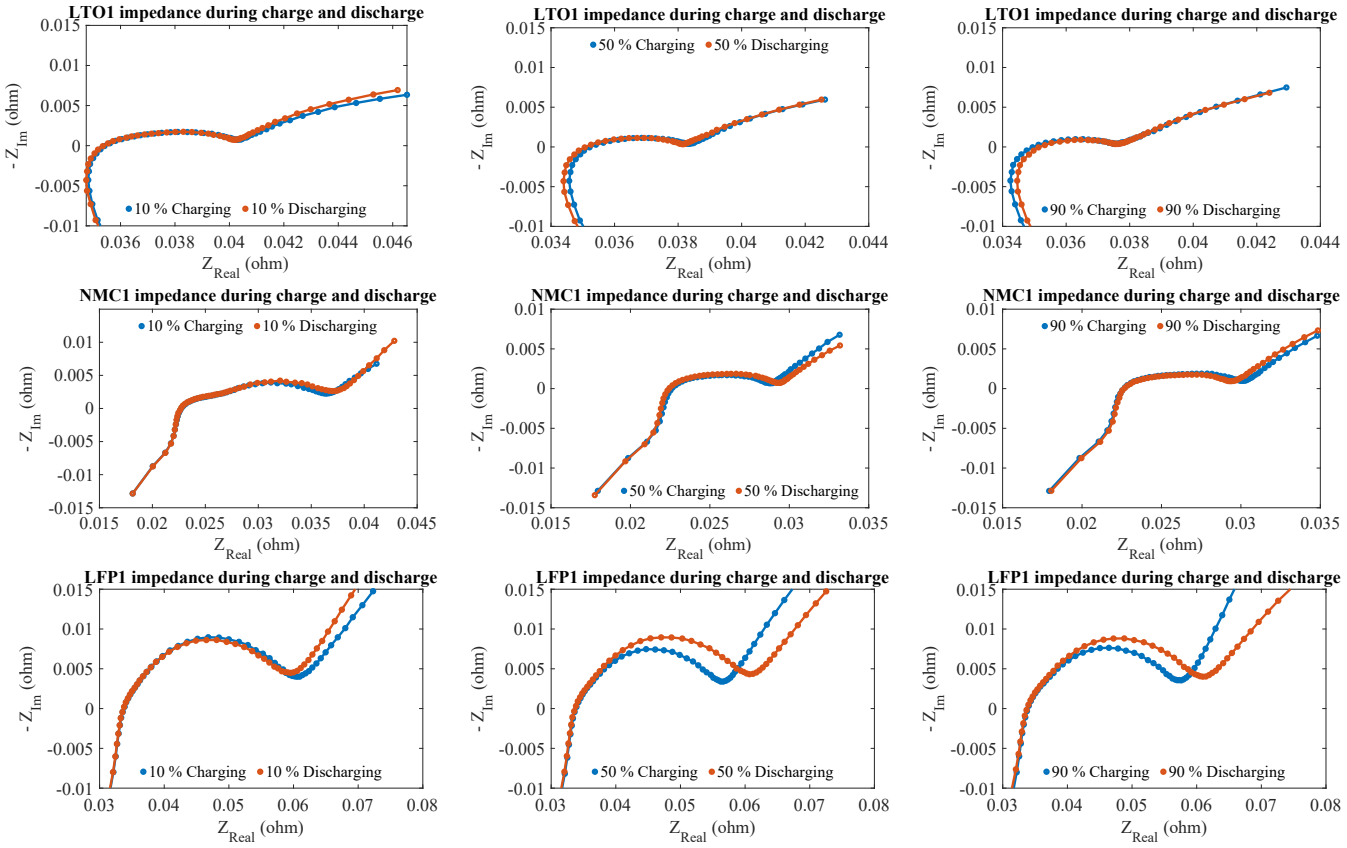

Fig. 20: Top: LTO impedance for different SoC during charge and discharge. Middle: NMC impedance for different SoC during charge and discharge. Bottom: LFP impedance for different SoC during charge and discharge

a) LTO

First, the impedances of the LTO battery cell were plotted, these can be seen on the top of fig. 20. Here we can observe that the graphs are almost identical. The only deviation on the 10% SoC graph can be seen in the low-frequency region, the right side of the plot, where the imaginary impedance during charging is lower. Note that the first point on the y-axis is 0.005 so this is a minimal difference which is negligible in this case. The other minor differences can be seen on the 90% and 100% SoC graphs, where the real impedance seems to be higher and lower during charging than discharging respectively. Once again, the reference point is about 0.035 on the x-axis, which is also negligible. Hence, the conclusion is that there is barely any influence on impedance when charging or discharging. This means that there is minimal or no hysteresis for an LTO cell.

b) NMC

For the NMC battery, the conclusion can be similar to what it was for the LTO. In the middle of fig. 20 one can see what the impedance plot looks like when measured during charge and discharge. We can see that the differences are minimal, there are two places where the plots do not overlap completely. These are on the 50% and 100% SoC plots. Here we can see that the imaginary impedance is somewhat higher for 50% SoC during charging. On the 100% SoC plot the opposite can be observed, the imaginary impedance is slightly lower during charging. Similarly to the LTO cell, these are insignificant differences as these deviations are in the range of ≈ 0.001 or even smaller for both cases. After all this, it can be stated that there is no big influence on impedance based on charging and discharging. Hence we can state that the hysteresis is minimal for an NMC battery cell.

c) LFP

The LFP is somewhat different from the previous two cells. We can see from the plots that there are significant differences between the impedances based on the charging direction. The direction does not influence the impedance at 10% SoC, the only small difference is at lower frequencies. In contrast, it is apparent that for middle and high SoC there are noteworthy differences. The two plots split around the first part of the mid-frequency region and from that point, they follow a completely different path. In the mid-frequency region, the imaginary impedance is higher during discharging. However, in the low-frequency region, this was switched, and the imaginary impedance was higher when charging. As for the real impedance, it can be seen that it is similar at the beginning, just like the overall impedance. After the two graphs split, the real impedance increases during discharge. Based on this analysis it is apparent that the hysteresis has a major effect on this battery type.

B. Equivalent circuit model

1) Choosing the ECM

There were three ECMs considered to be used to model the battery cells. The three circuits can be seen on fig. 21. On top of the figure, we can see the second-order RC pair, in the middle a circuit with one CPE and on the bottom a circuit with two CPEs. Using the software impedance.py it was possible to see how the simulated ECMs would compare with the measured data [26]. The software uses curve fitting by non-linear least squares regression. Moreover, an error plot was also plotted to see which ECM had less error during the fitting process. The 3 ECMs were tested for each of the three battery chemistries. As we established before the impedances were very similar enough for the cells regarding both charge direction, cell difference and SoC. Hence it was decided that for this part it is sufficient to use only one cell per chemistry and use the data from the discharging direction at a specific SoC. This means that only one cell's data during discharging will be used for every chemistry. However, it can be assumed

that the conclusions drawn from this process are true for the other cells and for charging too.

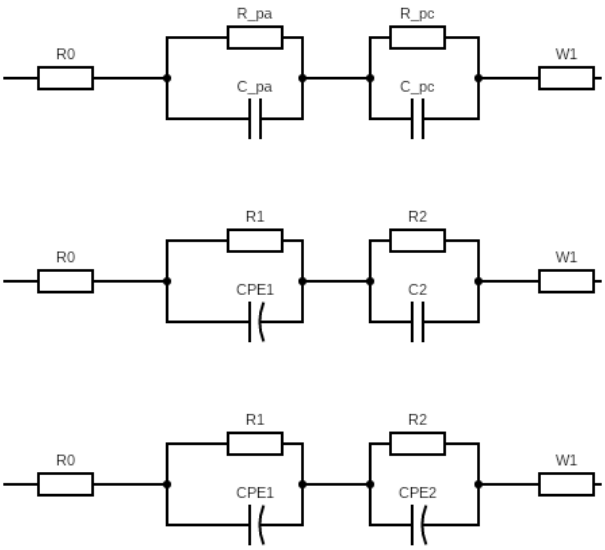

Fig. 21: The three options for ECM

a) LTO

First, the LTO battery cell, the chosen SoC, where the ECM testing will be performed, is 50%. The three possible ECMs were fitted and the error plot was plotted. On fig. 22, fig. 23 and fig. 24 we can see how these compare to each other and the actual measurement data with the error plot.

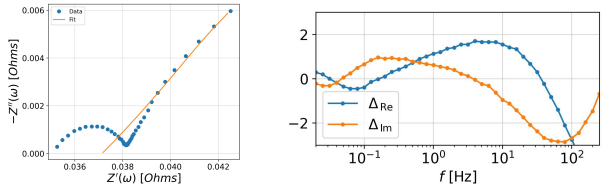

Fig. 22: Left: LTO impedance graph with first ECM option. Right: LTO error graph with first ECM option

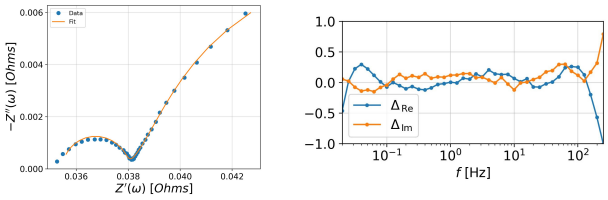

Fig. 23: Left: LTO impedance graph with second ECM option. Right: LTO error graph with second ECM option

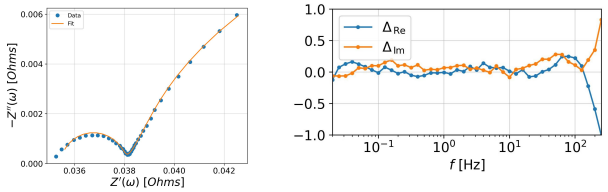

Fig. 24: Left: LTO impedance graph with third ECM option. Right: LTO error graph with third ECM option

It is clear that the first ECM option does not perform well at all, this means that this circuit is not appropriate to model an LTO cell. On the other hand, we can see that the two models with one and two CPEs have a good correlation between the measured and simulated data. This can be observed by looking at the impedance graphs where the plotted data is almost the same. To choose a preferable ECM, we have to look at the error plot of the second and third options. By looking at these plots we can see that the error is a bit better for the third ECM, it is a small difference only but still an important one. After the analysis of the results and the simulations, it is now safe to say that the ideal ECM out of the three is the third one, the circuit with two CPEs. The circuit can be seen on fig. 21.

b) NMC

Next, it is time to take a look at the NMC cell. The same process was completed as before. The plots of impedance and error for the three ECM options can be seen on fig. 25, fig. 26 and fig. 27.

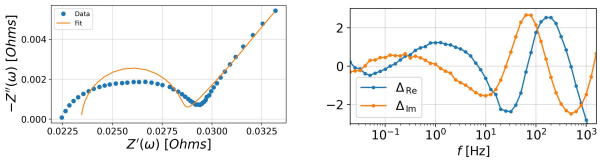

Fig. 25: Left: NMC impedance graph with first ECM option. Right: NMC error graph with first ECM option

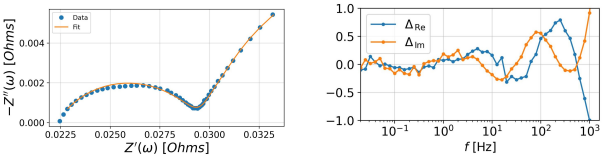

Fig. 26: Left: NMC impedance graph with second ECM option. Right: NMC error graph with second ECM option

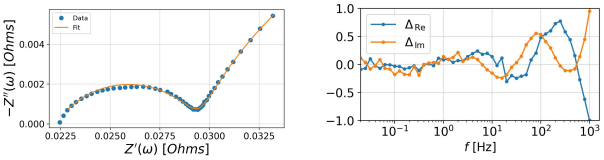

Fig. 27: Left: NMC impedance graph with third ECM option. Right: NMC error graph with third ECM option

By analysing the plots we can quite easily state that the second-order RC circuit (first option) is not going to be a good solution to model this type of battery. The impedance graph does not fit and the error plot is way too high for this ECM to be considered. Once again the circuits with one CPE and two CPEs produce very similar results. The impedance plot fits well and is almost the same for the two models. The only difference can be found in the error plots. Once more the model with two CPEs has a slightly smaller error in the low-frequency region, other than this the error is almost the same. The decision based on this is to select the third option as the ideal ECM, this circuit can be seen on the bottom fig. 21.

c) LFP

At last, the LFP plots for the different ECM options can be seen on fig. 28, fig. 29 and fig. 30.

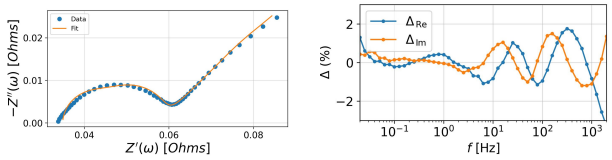

Fig. 28: Left: LFP impedance graph with first ECM option. Right: LFP error graph with first ECM option

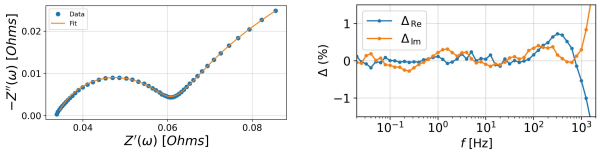

Fig. 29: Left: LFP impedance graph with second ECM option. Right: LFP error graph with second ECM option

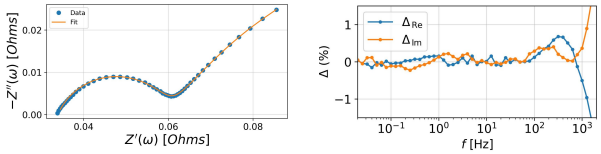

Fig. 30: Left: LFP impedance graph with third ECM option. Right: LFP error graph with third ECM option

It is apparent from the graphs that the first ECM option is not a good solution. The impedance graph does not fit well and the error is too high. On the other hand, the remaining two options seem like a good choice. They both fit the impedance curve remarkably well. Hence, once again the decision can be based on the error plot. We can see that the error plots are also similar, however by looking at them carefully we can spot minor differences. These favour the third choice ECM, the circuit with two CPEs. There are segments of the plots where the error is smaller for the circuit with two CPEs than the circuit with one CPE. Based on this analysis, we can say that the best option, out of the discussed three, is the fractional-order model. This circuit can be seen on fig. 21.

2) Verification of chosen ECM

The validation of the chosen ECM will be shown by showing multiple SoCs and their corresponding ECM circuit performance and these will be compared to the data from the actual measurement.

a) LTO

For the LTO cell the plots for 20%, 40%, 60% and 80% can be seen on fig. 31, fig. 32, fig. 33 and fig. 34 respectively.

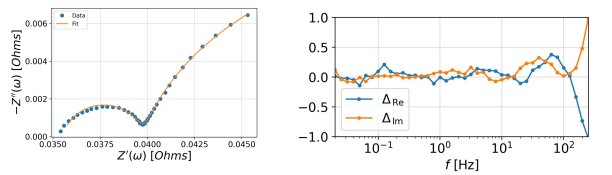

Fig. 31: Left: LTO impedance at 20% SoC. Right: LTO error at 20% SoC

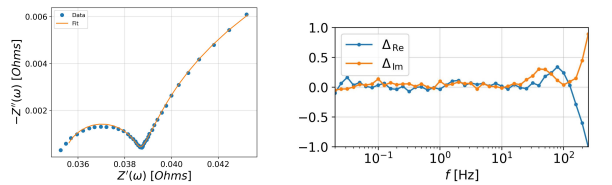

Fig. 32: Left: LTO impedance at 40% SoC. Right: LTO error at 40% SoC

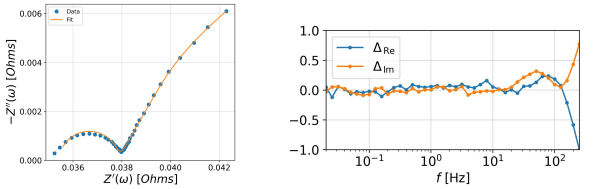

Fig. 33: Left: LTO impedance at 60% SoC. Right: LTO error at 60% SoC

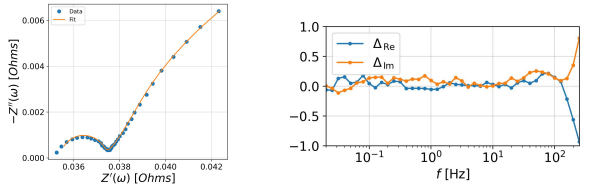

Fig. 34: Left: LTO impedance at 80% SoC. Right: LTO error at 80% SoC

By investigating the graph we can observe that the impedance graphs correlate very well for every SoC in terms of the measured data and simulated data. Looking at the error plots, it can be observed that the error is very small for every SoC. The reason for showing four different SoCs is to prove that the chosen ECM is a good choice for the whole range of the battery, as we can see that it performs exceptionally well for low, middle and high SoCs. A conclusion then can be that the model with two CPE is a good choice for an ECM if one would want to model an LTO battery cell. This choice would be a good choice for the whole range of the SoC and we can assume that it is not influencing the simulation if we charge or discharge.

b) NMC

Next, the validation of the NMC cell. The same simulations were performed with the ECM where there are two CPEs. On fig. 35, fig. 36 and fig. 37 one can see the impedance and error plots for 10%, 60% and 100% SoC respectively. We can see that for NMC there are significant differences between the ECM performance on specific SoCs.

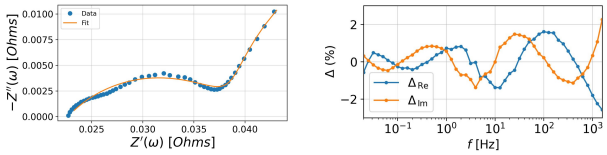

Fig. 35: Left: NMC impedance at 10% SoC. Right: NMC error at 10% SoC

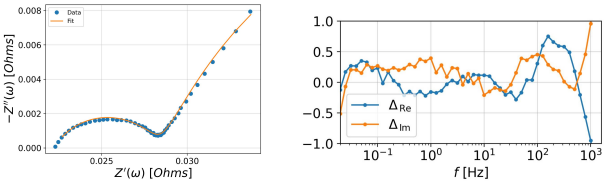

Fig. 36: Left: NMC impedance at 60% SoC. Right: NMC error at 60% SoC

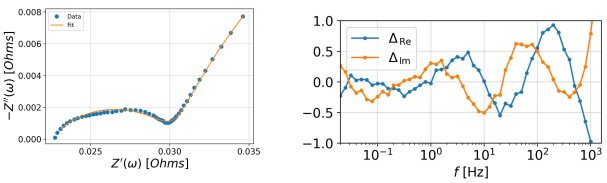

Fig. 37: Left: NMC impedance at 100% SoC. Right: NMC error at 100% SoC

We can see that the performance is not ideal for 10% and 100%. The simulated result fits the measured one, but the error rate is high. The performance for 60% is acceptable, the graph mostly fits well and the error is below 0.5%. One conclusion can be that the chosen ECM works for the middle range of the SoC. On the other hand, this ECM might not be the best choice to model the lower range $(0\% - 20\%)$ and very high range (100%) of SoC. As this ECM was deemed the be the best out of the three we can also assume that the other two options would also fail to meet an acceptable performance level. Therefore, to properly simulate this battery type, more research has to be done.

c) LFP

The verification of the chosen ECM for the LFP cell will be similar to the verification of the LTO, four different SoCs will be shown and compared. On fig. 38, fig. 39, fig. 40 and fig. 41 the plots of the four SoCs, namely 20%, 40%, 40% and 80%, can be seen.

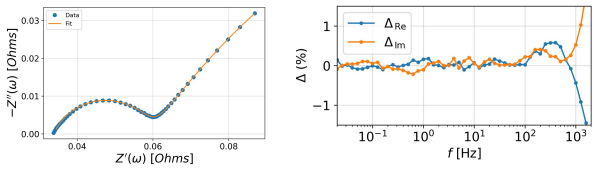

Fig. 38: Left: LFP impedance at 20% SoC. Right: LFP error at 20% SoC

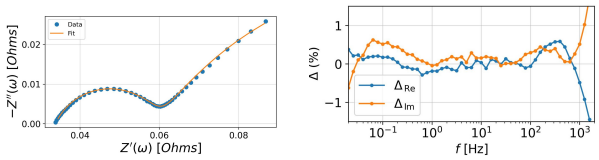

Fig. 39: Left: LFP impedance at 40% SoC. Right: LFP error at 40% SoC

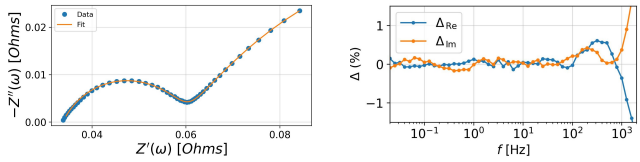

Fig. 40: Left: LFP impedance at 60% SoC. Right: LFP error at 60% SoC

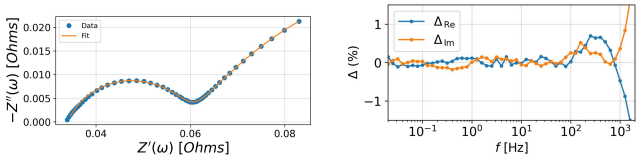

Fig. 41: Left: LFP impedance at 80% SoC. Right: LFP error at 80% SoC

By analysing the plots, we can see that the performance of the third ECM is satisfactory. The impedance plot fits generally well and the error is minimal for three of the four cases. It is necessary to analyse the 40% SoC plot further. The impedance plot fits well, so the difference can be found in the error plot. This difference is not too big in this case, however, it is apparent that the error is a bit higher than in the other cases. On the other hand, most of the error is still well below 1% for most of the simulation, which can be considered a good performance. Based on this, we can say that, even with a minor difference at 40% SoC, the ECM with two CPEs is a good solution to model an LFP battery cell. It performs effectively for the whole range of the SoC with minimal error.

VI. Conclusion

This paper focused on finding an optimal ECM for specific Lithium-ion battery cells by performing EIS measurements. Three different battery chemistries were investigated, LTO, NMC and LFP. The cells were probed to obtain their capacity and EIS measurements were performed to acquire an optimal current to work with. These currents were $80mA$ for LTO and NMC and $60mA$ for LFP. Measurements were performed to investigate the influence of SoC and charging direction on the impedance of the battery cells. From these measurements, conclusions were drawn regarding this influence. We can say that for LTO and NMC the charging direction does not influence the cell impedance. Hence we can say that there is no to minimal hysteresis for LTO and NMC cells. The SoC can influence the impedance of these cells. In both cases, we could see that at 100% and 0% the impedances are significantly different compared to other SoCs. Moreover, for LTO the real part of the impedance decreases as SoC increases. This trend can be observed for the NMC cell too, the real impedance decreases as the SoC increases. On the other hand, for the LFP cell, we could see that charging directions affect the cell impedance but the SoC does not. This means that hysteresis has a major effect on this battery type. Next, three different ECMs were simulated and compared with the measurement data. There were deviations between the ECMs as expected. The acceptable range on the error plots of these deviations, based on personal experience, was that the error is ideally below 0.5%. For the curve fitting it was easier to decide the range as we could see how the plots fit so it was clear which performance is acceptable and which is not. The simulation showed that the optimal ECM for the LTO cell is a circuit with two CPEs. The same circuit provided the best option out of the three for the NMC cell. However, it is suboptimal for certain SoC ranges, it turned out that from 0% to 20%, this circuit is not ideal to model this cell. Hence the conclusion is that there is a demand for more research to find an ECM that can properly simulate the NMC cell. This is potentially a good option for further research and work. Finally, for the LFP cell, the third ECM option could perform consistently well for the whole range of SoC. Hence, we found a suitable ECM for two of the three proposed battery chemistries and we found out that there is more work and research to be done to find an appropriate ECM for the NMC cell.

VII. Acknowledgment

I would like to thank my supervisors dr. ir. Prasanth Venugopal and Zhansheng Ning for their support and assistance during this project. I would like to thank Zhansheng Ning for his technical support with the usage of the lab equipment.

VIII. Declarations

During the preparation of this work, the author used Grammarly, Gemini, Citation Machine and ChatGPT; for help with writing, citation management, literature searching and improving text in order to deliver a professional and coherent-sounding text. After the use of these tools/services, the author reviewed and edited the content as needed and takes full responsibility for the content of the work.

References

[1] (n.d.) Lithium ion battery advantages & disadvantages. Electronics Notes. [Online]. Available: https://www.electronics-notes.com/articles/electronic_components/battery-technology/li-ion-lithium-ion-advantages-disadvantages.php

[2] (2022) Is lithium-ion the ideal battery? Battery University. [Online]. Available: https://batteryuniversity.com/article/is-lithium-ion-the-ideal-battery

[3] J. Fleischmann, M. Hanicke, E. Horetsky, D. Ibrahim, S. Jautelat, M. Linder, P. Schaufuss, L. Torscht, and A. van de Rijt. (2023) Battery 2030: Resilient, sustainable, and circular. McKinsey & Company. [Online]. Available: https://www.mckinsey.com/industries/automotive-and-assembly/

our-insights/battery-2030-resilient-sustainable-and-circular#/

[4] K. Gordon. (2023) Lithium-ion battery market to hit $184 billion by 2030; kmet captures. ETF Trends. [Online]. Available: https://www.etftrends.com/climate-insights-channel/lithium-ion-battery-market-to-hit-184-billion-by-2030-kmet-captures/

[5] (2021) What are lithium-ion batteries? UL Research Institutes. [Online]. Available: https://ul.org/research/electrochemical-safety/getting-started-electrochemical-safety/what-are-lithium-ion

[6] D. Deng, "Li-ion batteries: basics, progress, and challenges," *Energy Scinece & Engineering*, 2015.

[7] N. Nitta, F. Wu, J. T. Lee, and G. Yushin, "Li-ion battery materials: present and future," *Materials Today*, 2015.

[8] M. Akbarzadeh, J. De Smet, and J. Stuyts, "Battery hybrid energy storage systems for full-electric marine applications," *Processes*, 2022. [Online]. Available: https://www.mdpi.com/2227-9717/10/11/2418

[9] (2024) Top 5 lithium batteries for commercial energy storage. TROES. [Online]. Available: https://troescorp.com/top-5-lithium-batteries-commercial-energy-storage/#

[10] A. Väyrynen and J. Salminen, "Lithium ion battery production," *The Journal of Chemical Thermodynamics*, 2011.

[11] M. Li, J. Lu, C. Zhongwei, and A. Khalil, "30 years of lithium-ion batteries," *Advanced Materials*, 2018.

[12] S. Bhowmick. (2022) A detailed comparison of popular li-ion battery chemistries used in electric vehicles. Circuit Digest - Electronics Engineering News, Latest Products, Articles and Projects. [Online]. Available: https://circuitdigest.com/article/a-detailed-comparision-of-popular-li-ion-battery-chemistries-used-in-evs

[13] Y. Miao, P. Hynan, A. von Jouanne, and A. Yokochi, "Current li-ion battery technologies in electric vehicles and opportunities for advancements," *Energies*, 2019.

[14] M.-K. Tran, A. DaCosta, A. Mevawalla, S. Panchal, and M. Fowler, "Comparative study of equivalent circuit models performance in four common lithium-ion batteries: Lfp, nmc, lmo, nca," *Batteries*, 2021.

[15] C. Blanco, L. Sanchez, M. Gonzalez, J. C. Antón, V. García Fernández, and J. Viera, "An equivalent circuit model with variable effective capacity for lifepo4 batteries," *IEEE Transactions on Vehicular Technology*, 2014.

[16] M. Hu, Y. Li, S. Li, C. Fu, D. Qin, and Z. Li, "Lithium-ion battery modeling and parameter identification based on fractional theory," *Energy*, 2018.

[17] P. Iurilli, C. Brivio, and V. Wood, "On the use of electrochemical impedance spectroscopy to characterize and model the aging phenomena of lithium-ion batteries: a critical review," *Journal of Power Sources*, 2021.

[18] X. Wang, X. Wei, and H. Dai, "Estimation of state of health of lithium-ion batteries based on charge transfer resistance considering different temperature and state of charge," *Journal of Energy Storage*, 2019. [Online]. Available: https://www.sciencedirect.com/science/article/pii/S2352152X18305279

[19] Q.-K. Wang, Y.-J. He, J.-N. Shen, X.-S. Hu, and Z.-F. Ma, "State of charge-dependent polynomial equivalent circuit modeling for electrochemical impedance spectroscopy of lithium-ion batteries," *IEEE Transactions on Power Electronics*, 2018.

[20] H. Xiao, Z. Tao, H. Bai, H. Wang, Y. Fu, N. Si, and H. Bai, "State of charge effects on the parameters of electrochemical impedance spectroscopy equivalent circuit model for lithium ion batteries," *IOP Conference Series: Earth and Environmental Science*, 2020.

[21] A.-I. Stroe, J. Meng, D.-I. Stroe, M. Świerczyński, R. Teodorescu, and S. Kær, "Influence of battery parametric uncertainties on the state-of-charge estimation of lithium titanate oxide-based batteries," *Energies*, 2018.

[22] I. Baccouche, S. Jemmali, B. Manai, N. Omar, and N. ESSOUKRI BEN AMARA, "Improved ocv model of a li-ion nmc battery for online soc estimation using the extended kalman filter," *Energies*, 2017.

[23] T. Huria, M. Ceraolo, J. Gazzarri, and R. Jackey, "Simplified extended kalman filter observer for soc estimation of commercial power-oriented lfp lithium battery cells," *SAE International*, 2013.

[24] N. Meddings, M. Heinrich, F. Overney, J.-S. Lee, V. Ruiz, E. Napolitano, S. Seitz, G. Hinds, R. Raccichini, M. Gaberšček, and J. Park, "Application of electrochemical impedance spectroscopy to commercial li-ion cells: A review," *Journal of Power Sources*, 2020.

[25] (2024) Echemlab xm potentiostat galvanostat. AMETEK Scientific Instruments. [Online]. Available: https://www.ameteksi.com/products/potentiostats/single-channel/apps-xm-series/echemlab-xm

[26] M. D. Murbach, B. Gerwe, N. Dawson-Elli, and L. kun Tsui, "impedance.py: A python package for electrochemical impedance analysis," *Journal of Open Source Software*, 2020. [Online]. Available: https://doi.org/10.21105/joss.02349